Autonomous Cornering Control based on Sense of Circular Vision Model

Ren Degoshi, Hiroyuki Masuta, Youtaro Fuse, Tatsuo Motoyoshi, Kei Sawai, Myagmardulam Bilguunmaa, Noboru Takagi
Dept. of Intelligent Robotics
Toyama Prefectural University
Toyama, Japan
u354014@st.pu-toyama.ac.jp, {masuta, fuse, motoyosh, k_381, bilguunmaa, takagi}@pu-toyama.ac.jp

2024 IEEE International Conference on Fuzzy Systems (FUZZ-IEEE) | 979-8-3503-1954-5/24/$31.00 ©2024 IEEE | DOI: 10.1109/FUZZ-IEEE60900.2024.10611756

***Abstract*—Recently, Research and Development of technology are actively conducted in the automotive industry. When automated driving becomes widespread, it is important to have a vehicle control system that does not cause anxiety or discomfort to passengers. However, many people have concerns about comfort and safety of autonomous driving system. One factor is the difference between automated driving and human driving. In advanced driver assist system, autonomous driving controller is considered human perception based on "human" system design. However, autonomous cornering control doesn't consider human perception factors. In previous research, Kumano et al. defined the Sense of Circular Vision (*SoCV*) as a type of sensory information expressed by the visual stimulation of optical flow on the retina during cornering behavior. In this paper, we focus on the vehicle control based on the *SoCV* model. And we discuss what kind of driving characteristics according to the optical flow based visual feedback.**

Keywords— Autonomous-Vehicle, Anxiety, Optical Flow, Human Visual Information, Discomfort Perception

I. Introduction

A. Background

Recently, development and research of autonomous driving technology are actively conducted in the automotive industry. Autonomous driving technology is expected to drastically decrease traffic accidents and support transportation for elderly individuals. However, many people have concerns about comfort and safety of autonomous driving system [1]. Matuura etc., insists that one of the reasons is the difference between the driving style of autonomous driving behavior and human driving behavior [2]. An autonomous vehicle often focuses on the "automobile and environment" system, however "human system" which is considered a human being is important [3].

In advanced driver assist system, autonomous driving controller is considered human perception based on "human" system design. For example, an adaptive cruise control is controlled following distance based on the human perceived sense of approach model [4]. As a result, the discomfort of passenger is reduced. On the other hand, current autonomous cornering control like Lane Keep Assist System keeps a vehicle within the center of the lane according to GPS and map information. This autonomous cornering control doesn't consider human perception factors.

Generally, a driver uses various sensory organs to operate a vehicle based on the surrounding environmental information and vehicle behavior [5]. Especially, visual information is the most important. In the cornering control, a human mostly relies on the visual perception. This research is focused on the visual perception. This research is focus on the visual perception like human being in the cornering behavior.

B. Related Reserch

There is a lot of research related to visual information and driving. Optical Flow (OF) is the flow of light projected onto the human retina as defined by Gibson [6]. Drivers perceive future trajectory from OF[3][7][8]. Ino et al. insists that optical flow based autonomous driving is controlled similarly to the human expert driver [3]. Fig. 1 shows a conceptual image of the OF as perceived by the driver. The OF that is caused by the vehicle motion expands from the center of the front vision when a vehicle is approaching a corner. On the other hand, the flow due to eye movement is followed sideway. As a result, the OF on the retina expand from the corner ahead. This focus of expansion (FOE) corresponds to the expected position for arrival. Ino et al. insisted that a driver perceives the direction of their self-motion through the perception of this FOE [3].

Based on the above, the ideal trajectory was determined to ensure that the FOE is always aligned with the road. As a result, the FOE based controller showed the turning radius, showing that there is a wide range in the selection of the target point. Moreover, the trajectory created by the FOE based controller was similar to that driven by an expert driver [9]. However, Ino's approach is difficult to adapt to environmental changes, because determining the target trajectory relies on GPS and map information. To adapt to environmental changes,

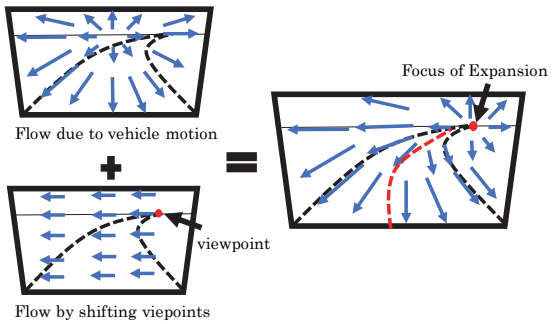

Fig. 1. Conceptual diagram of OF.

feedback control elements using camera images or other methods would be required. Therefore, we propose an autonomous cornering control including feedback elements that is calculated FOE using a camera image. In previous research, Kumano et al. defined the Sense of Circular Vision (*SoCV*) as a type of sensory information expressed by the visual stimulation of optical flow on the retina during cornering behavior [10][11]. We expect that ideal cornering control, which maintains a constant optical flow will be realized through feedback based on the output of the *SoCV* model. Therefore, the ideal cornering control aims to constantly maintain the *SoCV*. In this paper, we do not consider the implementation of the proposed method. Through simulation experiments, we evaluate the outcomes resulting from the application of this control.

II. Sensation of Circular Vision Model

A. The methods of Calculating OF

This section explains the *SoCV* as proposed by Kumano et al. The *SoCV* represents the detection of optical flow and FOE from the perspective projected onto the retina [10][11]. Section A describes how OF is calculated. To acquire information closely resembling the flow of light projected onto the human retina, we calculate OF through sensor and camera sensor fusion [10]. The extracted OF takes into account the lane boundaries, which are factors influencing human turning behavior, and computes the OF in the lane sections. The OF of the lane boundary projected on the retina is determined by the flow due to self-motion and the amount of viewpoint movement. The OF due to self-motion is calculated from the motion of the own vehicle to prevent noise. Equation (1) and (2) are calculated azimuthal direction $F_{\mathrm{Azi}}(t)$ and elevation direction $F_{\mathrm{ele}}(t)$of the OF.

$$F_{\mathrm{Azi}}(t) = \frac{\theta'(t) - \theta(t-1)}{\Delta t} \tag{1}$$

$$F_{\mathrm{Ele}}(t) = \frac{\varphi'(t) - \varphi(t-1)}{\Delta t} \tag{2}$$

θ[rad] is the azimuth angle in retinal coordinates. φ[rad] is the elevation angle in retinal coordinates. The flow due to the viewpoint shift is half of the yaw rate of the vehicle. The OF projected on the retina is obtained by subtracting the viewpoint movement flow from the OF due to self-motion (Fig. 1). From insights in related studies, a group of FOE candidate points that radiate from the center of the viewpoint is considered the self-motion direction perception by the driver. The Optical Flow (OF) around the FOE candidate points is oriented to the left when on the left side and to the right when on the right side [3].

B. Sensation of circular vision model

The previous study [3] is shown that the driver's perception of self-motion is related to the FOE that radiates from the center of the viewpoint. Thus, the ideally obtained OF on the white line should be bilaterally symmetric. The visual deviation from this ideal state is defined as the Sense of Circular Vision (*SoCV*).

On the other hand, it is difficult to evaluate the acquired OF equally on the left and right sides, because the directions, magnitudes and densities of the OFs are different. The number of OFs on the outside white line is greater than on the inside, and the flows on the near side have a larger magnitude than those on the far side in a curve. To evaluate OFs uniformly, a spiking neural network (SNN) is applied to be considered as a simulation on the retina.

The spike response model is applied for the SNN to evaluate OFs [12]. Fig. 2 shows an overview of the neurons used in SNN. A flow neuron is placed on the lane boundary at every 0.035 [rad] step for elevation angles ranging from 0 ~ -0.52 [rad]. The number of flow neurons at the left and right lane boundaries are N_{L} and N_{R}. Moreover, speed neurons and yaw rate neurons are placed to input the vehicle speed V [m/s] and the yaw rate γ [rad/s], respectively.

Equation (3) shows the environmental inputs to the flow neuron $h_i^{ext,FN}$. It takes as input the azimuthal direction of the lane boundary OF $F_{\mathrm{Azi},i}$[rad/s].

$$h_i^{ext,FN}(\mathrm{t}) = k \cdot F_{\mathrm{Azi},i} \tag{3}$$

k is an arbitrary constant. In flow neurons, inputs are given so that the firing frequency of the neuron increases when flow occurs in the ideal direction. The speed and yaw rate are normalized using a Gaussian membership function, and then inputted into each neuron.

The SNN connects to all neurons and learns based on the Hebb rule, which is expected to reduce noise effectively and predict changes in flow. However, the learned weight parameters are updated for each driving situation, therefore they cannot adapt to various situations. To adapt to various situations, multi-layered Neural Network (MNN) are used to maintain the learning weight parameters of the SNN for each situation. Fig. 3 shows the relationship between SNN and MNN. The inputs of MNN are curvature rate, vehicle speed and yaw rate, and the outputs are all weight parameters of SNN. The training, validation, and test data sets for training were obtained by randomly setting the vehicle speed, curve

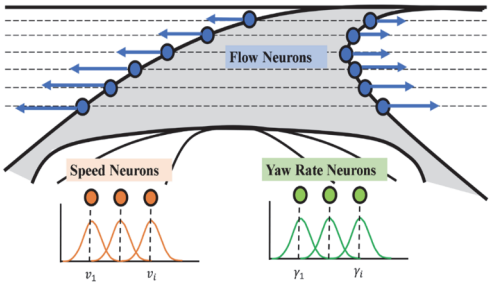

Fig. 3. overview of the neurons used in SNN.

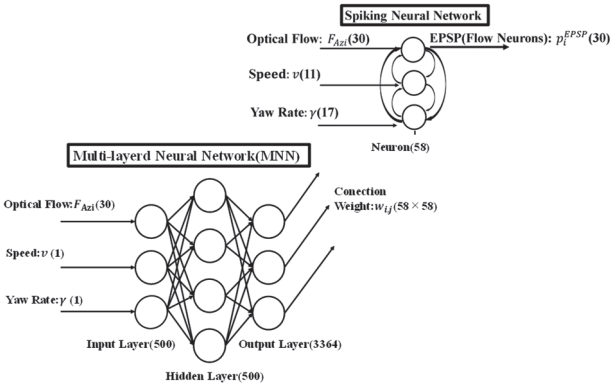

Fig. 2. overview of SNN and MNN.

curvature radius, and turn radius and turning radius for a simulation of driving from straight ahead to the end of the road in a curve. The vehicle speeds ranged from 9 to 21 [km/h], and the turning radius ranged from 10 to 50 [m]. The MNN learns SNN weights. The MNN overwrite the SNN weights corresponding to the facing situation.

Finally, the evaluation value of each lane boundary is calculated. The *SoCV* is defined as the difference in each evaluation value like Equation (4).

$$SoCV = \frac{\sum_{i=1}^{N_L} p_{i,L}^{EPSP}}{N_L} - \frac{\sum_{i=1}^{N_R} p_{i,R}^{EPSP}}{N_R} \quad (4)$$

N_L and N_R are the number of neurons on the left and right while lines, $p_{i,L}^{EPSP}$ and $p_{i,R}^{EPSP}$ are the output of the *i*-th neuron at each lane boundary. The *SoCV* is close to 0 when the flows on the left and right are equally expanded in the view. On the other, the *SoCV* has positive or negative value when the flows on the left and right are unequally expanded. This means that the FOE is placed the outside of the road area.

III. Vehicle Control Model

In this chapter, we propose the cornering control system based on the *SoCV* model. Fig. 4 shows the conceptual diagram of the cornering control system. The meaning of symbols in Fig. 4 are shown in Table. 1.

A. The conceptual diagram of the cornering system

In Fig.4, there are three major units: the autonomous cornering control unit, the vehicle control unit, and the vehicle model unit. The vehicle model unit calculates the vehicle's condition based on the input of the target torque on the drive shaft and the target steering angle using a 2-axle vehicle model in MATLAB/Simulink [13]. The vehicle control unit is a PI feedback controller for speed control, which outputs the target torque from the target speed, and for steering angle control, which outputs the target steering angle from the target yaw rate.

The autonomous cornering control unit outputs the target speed and the target yaw rate using fuzzy control and Model Predictive Control (MPC), respectively.

B. Model Predictive Control in the Autonomous cornering control unit

This section explains that the target yaw controller using a model predictive control to decide the target trajectory. The objective of this controller is to find the target yaw rate that achieves the minimum *SoCV* value. Fig. 5 shows a processing procedure to find the target yaw rate value. To achieve the

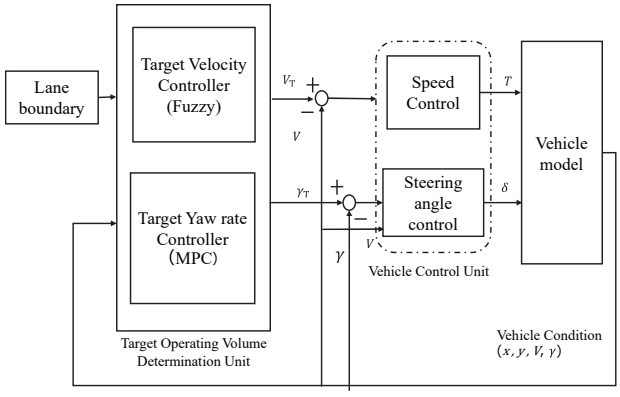

Fig. 4 the overall diagram of the control model.

TABLE I. Vehicle Parameters

x, y	**Vehicle Position [m]**
V	**Vehicle Speed [m/s]**
V_{T}	**Target Speed [m/s]**
γ	**Vehicle Yaw rate [rad/s]**
γ_{T}	**Target Yaw rate [rad/s]**
δ	**Steer Angle [rad]**
T	**Torque [N・m]**

minimum *SoCV* along the target trajectory, it is necessary to consider the future changes in *SoCV*, focusing not only on the current state but also on the anticipated future state.

Model Predictive Control (MPC) is a control method that predicts the future behavior of a control target based on observations and models, and then finds the optimum control input under a given evaluation function [14]. MPC (Model Predictive Control) can integrate and optimize both feed-forward and feedback control, making it well-suited for representing human behavior. Similarly, a human driver determines the operation by considering the future state, while also observing the current situation and the behavior of the vehicle[14]. The inputs are the lane boundary information from the environment, and the vehicle condition of the vehicle position, yaw angle, speed and yaw rate. Using these input data, a total *SoCV* for a trajectory is calculated based on a candidate yaw rate and at a constant speed. The total *SoCV* of a trajectory is the evaluation function *J* is shown in equation (4).

$$J_i = \sum_{t=0}^{tp} SoCV(t)^2 \quad (4)$$

where $t_p$is the prediction execution time. *i* represents the *i*-th number in the series of target yaw rate candidates. The execution time denoted as *t* is measured from the current position to t_p in increments of 0.1 seconds.

The target yaw rate candidates denote as γ_{i} are defined as values ranging from $\pm$ 0.3[rad/s] relative to the current yaw rate $\dot{\theta}$, in increments of 0.01 [rad]. Finally, the target yaw rate is chosen from the yaw rate candidate that has the minimum *Ji*, as described in Equation (5).

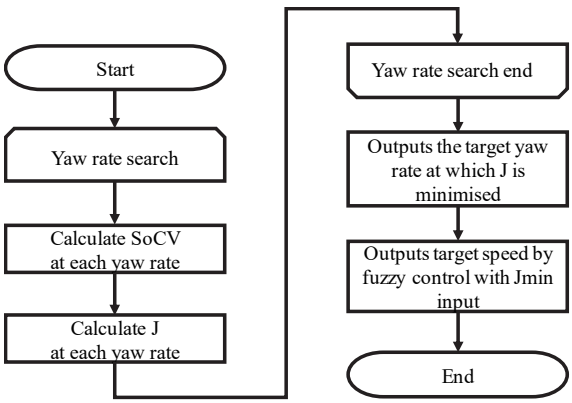

Fig. 5 the overall diagram of the control model.

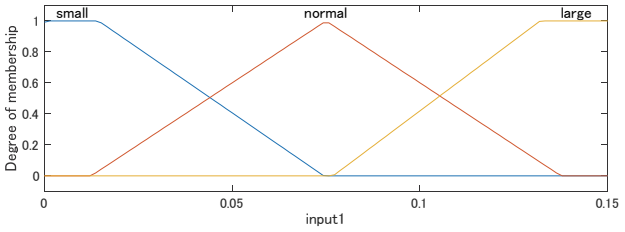

Fig. 6(a) the overall diagram of the control model.

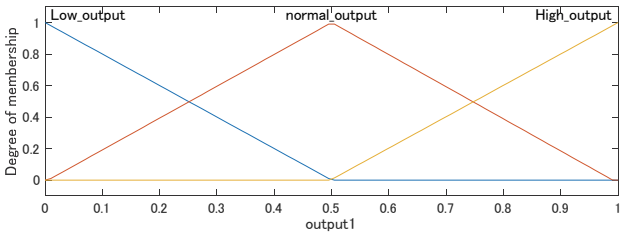

Fig. 6(b) the overall diagram of the control model.

Fig.6 the Functionship

$$\gamma_{\mathrm{T}} = \mathrm{argmin}(J_i) \tag{5}$$

C. *Fuzzy Control in the Autonomous cornering control unit*

This section describes the longitudinal motion control method for vehicles. As shown in Fig. 4, longitudinal motion control is performed by calculating the target speed using fuzzy control. Therefore, we considered that fuzzy control can be used for longitudinal motion control to smooth out changes in velocity. The output for determining the target speed is calculated based on the MPC evaluation function J in order to consider the dynamics of the turning sensory model output value *SoCV*. To determine the optimal value including the entire prediction interval, the minimum term of the target speed is determined using J_{min} as input. Fig. 6 shows the membership function for fuzzy inference. Fig. 6 (a) shows the membership function for the input J_{min}. Fig. 6 (b) shows the output. The minimax center-of-gravity method is used to determine the numerical values. Fuzzy outputs μ are output as 0~1. The target yaw rate is calculated by the output μ.

IV. Experiment by Simulation

This chapter presents the experimental results. Section A provides an overview of the simulation. Subsequently, Sections B and C describe the simulation results and the discussion, respectively. We assume a single apex corner as shown in Fig. 7 for our simulation.

A. *Simulation overview*

Fig. 7 shows the driving course used in the simulation. This course is composed of straight sections and corners with an apex radius of 40 meters. The road width is 3.5 meters. However, a relaxation curve is not set at the junctions between the straight sections and curves. The simulation environment was created using the MATLAB/Simulink Automated Driving Toolbox. The Automated Driving Toolbox provides algorithms and tools for designing, simulating and testing ADAS and automated driving systems[15].

This simulation performs three cases, the first with the vehicle speed constantly at 30 km/h without speed control (Case 1), the second with the vehicle speed constantly at 60 km/h without speed control (Case 2), and the third with an The purpose of this simulation is to consider visual information from the verification of driving characteristics of

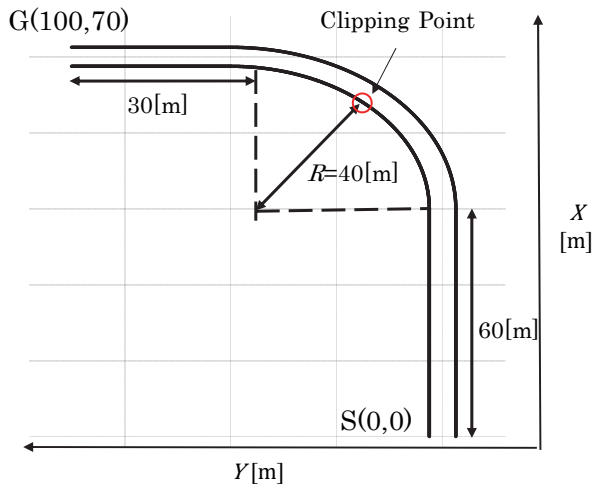

Fig. 7 the curse of simulation.

a vehicle control system using the Sense of Circular Vision model *SoCV*.

This simulation is performed by simulating running at a velocity of 30 [km/h], constantly running at a velocity of 60 [km/h], and finally running at an initial velocity of 60 [km/h], with velocity control. The predicted interval t_p was set to 1.5 seconds.

Through the simulation, we verify the characteristics of the vehicle's motion based on the *SoCV*. Our proposed method considers only the visualization of the front vision flows, not the road layout. Therefore, we focus on the running trajectory and the condition of the vehicle.

B. *Simulation results*

Fig. 8, Fig. 9, and Fig. 10 show the simulation results for Case 1, Case 2, and Case 3, respectively. In Fig. 8 and 9, (a) to (e) illustrate the acquired trajectory, measured X-Y position, acceleration, yaw rate, and *SoCV*, respectively. In Fig. 10, (a) to (f) illustrate the acquired trajectory, measured X-Y position, velocity, acceleration, yaw rate, and *SoCV*, respectively. In Fig. 8, the vehicle begins to turn the steering wheel at 6 seconds from the start, just before the corner. Subsequently, the *SoCV* increases from t=6 [s] to t=8.5 [s], reaching a maximum value of 0.04. Afterwards, both acceleration and yaw rate increase, but the *SoCV* approaches 0. The trajectory shows that the vehicle moves closer to the inner side of the corner, similar to human driving behavior.

In Fig. 9, the vehicle deviates from the course at t = 4.5 [s]. Generally, it is not safe for a vehicle to run at R = 40 [m] and V = 60 [km/h]. The vehicle deviates from the road at t = 4.5 [s], leading to a considerable increase in the *SoCV*. This implies that a human would experience strong visual stimulation upon deviating from the road, corresponding to the *SoCV* of about 0.1. Yaw rate and lateral acceleration are significantly increased. This means that the vehicle is trying to turn the corner to match the curvature, however the vehicle cannot turn properly due to excessive speed.

In Fig. 10, the vehicle completes a course even if the speed is 60 [km/h]. In Fig. 10, the vehicle completes a course even at a speed of 60 km/h. Fig. 10(c) shows that the speed decreases 2 seconds before the corner, and then increases from 8.4 [s] until the end of the corner due to the action of the speed

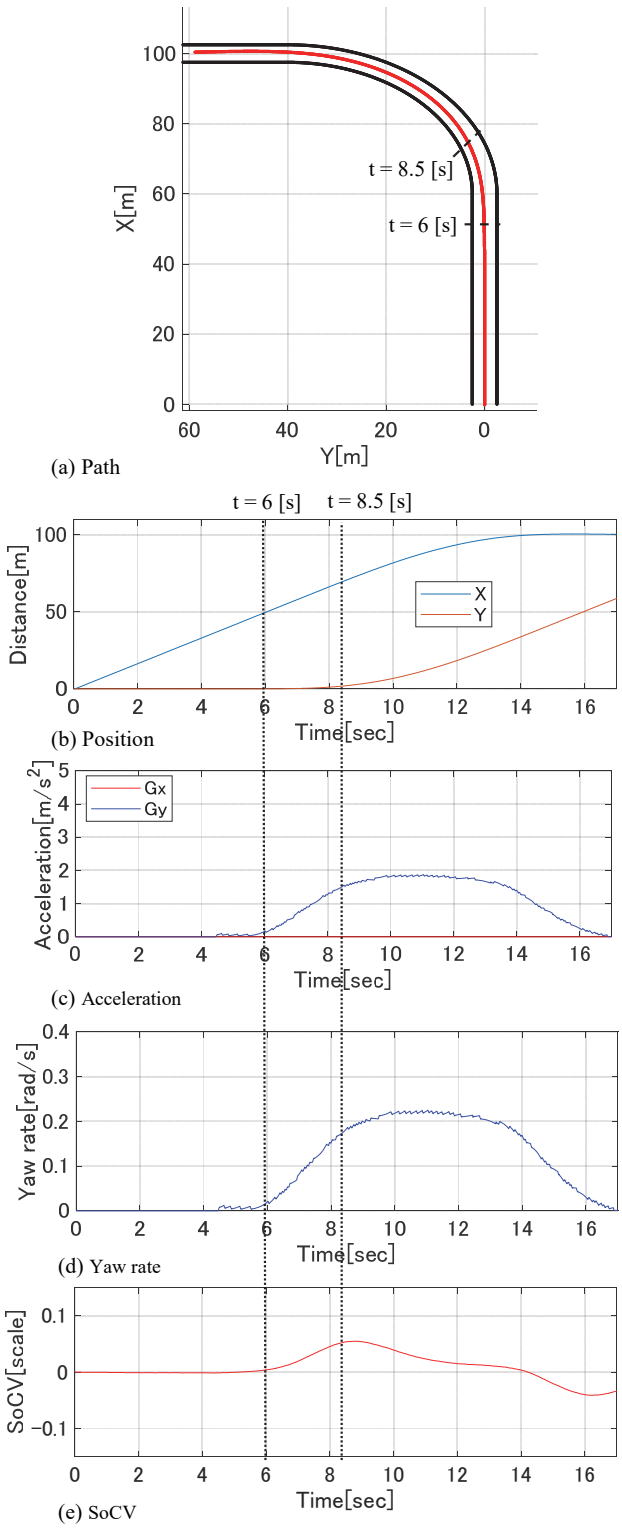

Fig. 8 results of simulation (Case 1)

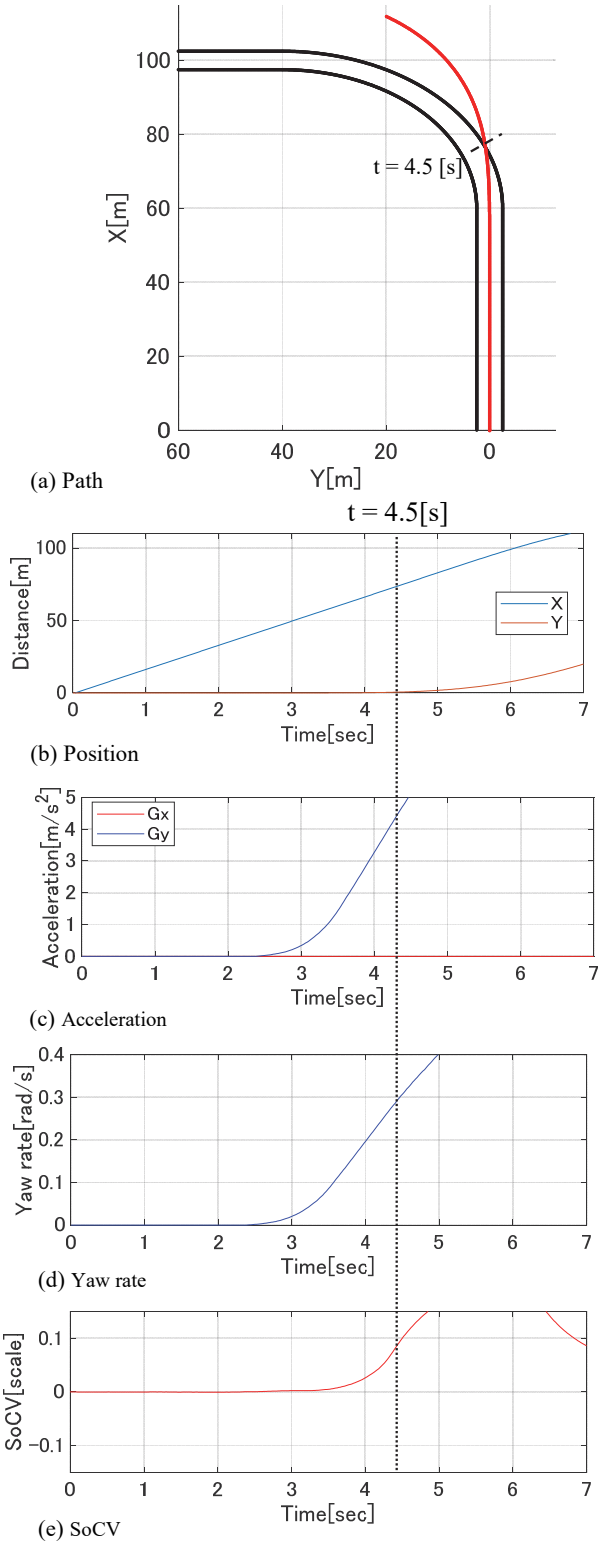

Fig. 9 results of simulation (Case 2)

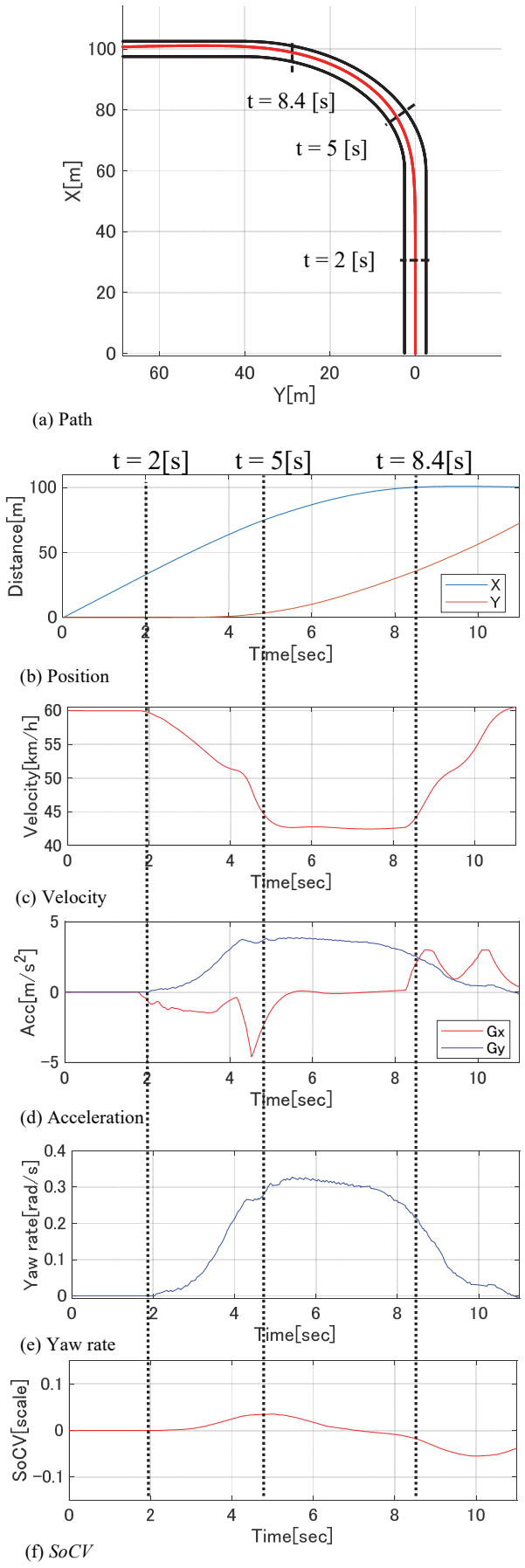

Fig. 10 results of simulation (Case 3)

controller. Simultaneously, the yaw rate increases in synchronization with the speed change starting at 2 seconds, as shown in Fig. 10(d). The cornering control begins earlier than Case1 due to the higher speed. The *SoCV* has a maximum value 0.06 at t=5 [s]. The area of highest visual stimulation is the approaching zone in the corner.

C. *Discuss simulation result*

In this section, the discussion performs the relationship between the *SoCV* and driving characteristics comparing with each case. In the driving trajectory of Fig. 8(a) and Fig. 10(a), both vehicle trajectory traveled with a relaxation curve before the corner.

From the driving paths shown in Fig. 8(a) and Fig. 10(a), it was confirmed that the yaw rate changed before the corner. This indicates that the vehicle is traveling with a relaxation curve before the corner. The vehicle moves closer to the inside area at the approach of the corner and then shifts towards the outside area at the end of the corner, depending on the vehicle speed. While on the corner, the flow on the outside is larger than on the inside. Therefore, the vehicle moves closer to the inside to achieve the *SoCV* closer to 0. In addition, the vehicle speed decreases before the corner and increases at the end of the corner. Since the *SoCV* cannot be reduced to below 0.1 with yaw rate control alone, the speed is decreased before the corner.

These vehicle behavior characteristics are very close to those of human operation from related studies[3][9]. The SoCV model considers only the optical flow on the retina during cornering, without taking the road layout. Nevertheless, the vehicle takes a behavior similar to human driving. The behavior of a human driver may be more influenced by visual perception than by knowledge of the driving environment.

In the experiment, t_p is set to 1.5 [s]. This indicates that the vehicle considers a maximum distance of 25 [m] ahead in the case of Fig. 10. Consequently, anticipatory behavior is provided to achieve the minimum value of *SoCV*. Ecological studies said that a human perceives the approaching time to the target about 1.2 to 2.0 [s] before [15]. This feature contributes to the similarity with the "smooth-running" characteristic of human driving. Therefore, the prediction time range is important to similar the human driving. However, actual road conditions and other disturbances may also have an effect. We will discuss this prediction range in the future research.

V. Conclusion

Many people have concerns about comfort and safety of autonomous driving system. One factor is the difference between automated driving and human driving. In advanced driver assist system, autonomous driving controller is considered human perception based on “human” system design. However, autonomous cornering control doesn’t consider human perception factors. In previous research, defined the Sense of Circular Vision (*SoCV*) as a type of sensory information expressed by the visual stimulation of optical flow on the retina during cornering behavior. In this paper, we focus on the vehicle control based on the *SoCV* model. And we discuss what kind of driving characteristics according to the optical flow based visual feedback. As a result, the vehicle control by the *SoCV* approached human driving characteristics. Human driver behavior may be

influenced more by visual perception than by knowledge of the driving environment.

In the future, we will discuss the prediction range of the model prediction for use in real environments. Moreover, we will conduct simulations in a double apex corner that simulate a real environment.

REFERENCES

[1] Liljamo, T., Liimatainen, H., Pöllänen, M., “Attitudes and concerns on automated vehicles,” Transportaition Research Part F: Traffic Psychology and Behaviour, vol. 59, pp. 24-44, 2018

[2] Matuura, T., Satou, K., “Classification and countermeasures for anxiety in driving based on clinical psychology,” Journal of Autonomous Vehicle Technology, Vol. 48, No. 4, pp. 141-146, 2017.

[3] Ino, H., Fukao, T., “Modeling of Driver Steering Operation Based on Optical Flow (Second Report)”, Transactions of Society of Automotive Engineers of Japan. 2014, Vol.45, No.4, p.711.

[4] Morita, K., Ono, T., Sekine, M., "Does Time-To-Collision Determine Brake Operation Timing" Proceedings of the 4th ITS Symposium, pp. 2-5, 2005.

[5] Kishida, H., Matsuzaki, N., Uenuma, K., “Study on Device Controlling Visual Information to Improve Driver's Performance”, Transactions of the JSME,2008, Vol.75, No.745, pp.2254-2263.

[6] Gibson, J.J, ” The perception of the visual world Hougtton Mifflin”, 1950

[7] Ino, H., Fukao, T., “Modeling of Driver Steering Operation Based on Optical Flow (Second Report)”, Transactions of Society of Automotive Engineers of Japan. 2014, Vol.45, No.4, p.711.

[8] Ino, H., Fukao, T., Totsuka, S., et al., “Development of Steering Control System Based on Optical Flow Model”, Transactions of Society of Automotive Engineers of Japan. 2015, Vol.46, No.2, p.443.

[9] Takahashi, A., Akiyama, Y., Hiraga, N., Hasegawa, Y., Yamakado, M., " Study of Steering Control Model Based on the Expert Driver's Behaviour", Transactions of Society of Automotive Engineers of Japan, Vol. 50,No.1,pp.102-108, 2019.

[10] Kumano, Y., Masuta, H., Motoyoshi, T., Sawai, K., Takagi, N., "Proposal of Optical Flow Calculation Method Using Celestial Sphere Camera during Vehicle Turning",Proceedings of the 36th Fuzzy SystemSymposium,2020.

[11] Degoshi, R., Masuta, H., Fuse, Y. Motoyoshi, T. Sawai, K., Takagi, N., “Development of Optimal Turning Control Using a Turn Sensation Model Based on Optical Flow for Autonomous Driving”, The 31st Intelligent Systems Symposium 2023, FAN2023, Fr-C2, 2023

[12] Wolfgang, Maass, Christopher M. BISHOP: Pulsed neural networks, MITpress,2001.

[13] MathWorks, “Modeling of Vehicle Motion Systems” https://jp.mathworks.com/help/ident/ug/modeling-a-vehicle-dynamics-system.html

[14] A. Koga, et al.: “Personalized autonomous driving using model predictive control : parameter estimation of personalized cost function”, International Journal of automotive engineering (IJAE), Vol. 47, No. 6, pp. 1431-1437 , 2016

[15] MathWorks, “Get Started with Automated Driving Toolbox”, https://mathworks.com/help/driving/getting-started-with-automated-driving-toolbox.html?lang=en (2024-4-30)

[16] M. Kondo, “Fundamental Relationship between Steering and Motion of Automobiles”, Transactions of Society of Automotive Engineers of Japan, No.5, pp. 40-43, 1958.